Drought Variability and Trends over the Central United States in the Instrumental Record

KINGTSE C. MO

NOAA/NWS/NCEP/Climate Prediction Center, College Park, Maryland

DENNIS P. LETTENMAIER

Department of Geography, University of California, Los Angeles, Los Angeles, California

(Manuscript received 28 November 2017, in final form 1 May 2018)

ABSTRACT

We examined drought variability and trends over the last century (1916–2013) over the conterminous United States (CONUS) using observed precipitation *P*, temperature *T*, and reconstructed total moisture percentiles (TMP) and runoff from four land surface models. We used an integrated drought index (IDI), which we defined as the equally weighted mean of the 3-month standardized runoff index (SRI3) and TMP from four land surface models mapped onto a uniform probability distribution. Using a definition of drought as IDI less than 0.3 for 6 months or longer, we identified 16 drought events, which we termed great droughts that covered more than 50% of the CONUS during our study period. We examined the properties of great droughts and compared these with the 2012 event. The great droughts were located at least partially over the central United States (30°–42°N, 85°–110°W). We found that 12 of these great droughts occurred when cold sea surface temperature anomalies (SSTAs) were located in the tropical Pacific with warm SSTAs in the North Atlantic. We also found a predominance of decreasing trends in IDI; droughts occurred less often and events were less severe as time progressed. In particular, only 2 of the 16 great droughts (2012 and 1988) occurred in the second half of the record.

1. Introduction

Shortages of water, commonly known as droughts, are among the most costly natural disasters (Wilhite 2006). Through 2011, Smith and Katz (2013) estimated that almost one-quarter of U.S. national hazard costs were associated with drought. The most recent costly ($1 billion or more) event was the 2012 drought and heat waves in the central United States. Aside from its severity, the 2012 drought was widespread; at its peak, it covered more than 62% of the conterminous United States (CONUS). The estimated cost of the 2012 event was about $40 billion, most of which was associated with lost agricultural production (https://www.rma.usda.gov/data). The large losses resulted in part because the event was not captured by the U.S. Drought Monitor (USDM) until mid-June and was not predicted by the Drought Outlook (http://www.drought.gov) until July, when drought was already well established. Therefore, water resources managers did not have an opportunity for advance mitigation of the impacts of the drought. Motivated by the 2012 drought, our objective here is to examine widespread droughts similar to the 2012 drought. We defined widespread droughts that covered over 50% of the CONUS as great droughts. Was the 2012 great drought an isolated event? How often did great droughts occur in the last century?

The 2012 drought was attributed to internal atmospheric variability by Hoerling et al. (2014). This implies that it could not be predicted by using either remote climate predictors, such as forecasted global sea surface temperature (SST) patterns, or by local land surface conditions such as soil moisture (Livneh and Hoerling 2016). There remains an important question of whether past great droughts over the central United States were mostly attributable to internal atmospheric variability. Past work seems to suggest otherwise; Schubert et al. (2004) attributed long-term droughts over the Great Plains (included in our definition of the central United States) to cold SST anomalies (SSTAs) in the tropical Pacific. Over the central United States, moisture is transported mostly by the low-level jet from the Gulf of Mexico (Mo et al. 1997). That transport is modulated by

Corresponding author: Dr. Dennis P. Lettenmaier, dlettenm@ucla.edu

DOI: 10.1175/JHM-D-17-0225.1

the atmospheric circulation that is often associated with SSTA forcing.

Drought variations over the central United States are modulated by ENSO (Ropelewski and Halpert 1986, 1989; Hu and Huang 2009; Cayan and Redmond 1994) at the interannual time scales within a decade. On decadal time scales, SSTAs in the North Pacific, the Pacific decadal oscillation (PDO), and the Atlantic multidecadal oscillation (AMO) can influence precipitation P directly (McCabe et al. 2004, 2008; Nigam et al. 2011; Coats et al. 2015) or indirectly by modulating the impact of ENSO on P (Schubert et al. 2009; Mo et al. 2009; Gershunov and Barnett 1998). The interesting question is what percentage of great droughts over the central United States are forced, and what are the forcings that initialize and maintain these great droughts? At decadal time scales, Cook et al. (1999) and Cook et al. (2014a,b) found by using paleo reconstruction methods that droughts over the last millennium were likely forced by SST forcings such as ENSO, AMO, and PDO. They also suggested the contributions from local forcings or local dynamics played a role. These forcings could act together or by themselves.

Andreadis and Lettenmaier (2006) studied soil moisture (SM) and runoff (RO) trends in the twentieth century over the CONUS and found that, with the exception of the Southwest and a small portion of the broader western United States, the CONUS has become wetter, with droughts occurring less often and having reduced severity in recent decades. These trends are consistent with increases of P over most of the CONUS as observed by Groisman et al. (2004) and Lettenmaier et al. (1994). An obvious question having to do specifically with great droughts over the central United States such as the 2012 event is whether they have become less frequent as well. If so, what are the reasons for the change? Is it due to changes in forcings?

Motivated by the above, our objective here is to identify great droughts over the CONUS over the last century and to identify trends and forcings. While there were many studies of the 2012 drought event (e.g., Rippey 2015; Cook et al. 2014b; Hoerling et al. 2014; Fuchs et al. 2015), there are few studies of the great droughts that covered more than 50% of the CONUS. We examine here 1) whether the 2012 drought was an isolated event, and how typical the 2012 event was in the context of the entire record of such events; 2) properties of historic great drought events; 3) the SSTAs associated with great droughts over the period of instrumental record; and 4) whether there were trends in the frequency of occurrence of great droughts.

We discuss the data used in section 2. In section 3, we examine spatial preferences of drought occurrence and long-term trends in drought indices. In section 4, we study historical great drought events. We further discuss and interpret our results and conclude in section 5.

2. Datasets and drought indices

Drought is usually defined in terms of drought indices, of which there are many (Keyantash and Dracup 2002). Meteorological drought usually is defined using precipitation P deficits measured by standardized precipitation indices (SPIs; McKee et al. 1993, 1995). Hydrological drought is defined by runoff or streamflow deficits while agricultural drought is defined by the lack of SM. There are only limited SM data available directly from observations and they do not cover much of the CONUS, so we rely instead on outputs from land surface models (LSMs) for SM and runoff.

a. LSM datasets

The forcing variables for LSMs include daily P, downward solar and longwave radiation, vapor pressure, as well as average temperature T [see Bohn et al. (2013), and references therein, for discussions of how these variables can be estimated from daily temperature maxima and minima and precipitation]. In addition, the models require daily (or in some cases subdaily) wind speed, which we took from the lowest vertical level of the NCEP–NCAR reanalysis (Kalnay et al. 1996) interpolated to 0.5° spatial resolution. Prior to 1950, we used seasonal averages of the post-1950 wind data. Livneh et al. (2013) showed that this had relatively little effect on predicted hydrologic state variables (e.g., soil moisture) and fluxes (e.g., runoff). The P and T observations were gridded from a set of nearly 2400 index stations over the CONUS as described by Wang et al. (2009). The gridding process (to 0.5° latitude–longitude spatial resolution) produces data records that are continuous and consistent through the study period. Our study period is from 1916 to 2013.

We ran the four LSMs and archived total column SM, snow water equivalent (SWE), and runoff from each. The four models we used were Noah 2.7 (Ek et al. 2003; Mitchell et al. 2004), VIC 4.0.6 (Liang et al. 1994), SAC-SMA (Burnash et al. 1973), and Catchment (Koster et al. 2000; Ducharne et al. 2000). Details of the LSMs are described in the above references; however, of particular relevance to this study are that the Noah model has four soil layers with fixed depths (total soil depth 2 m); the VIC model has three soil layers, the depth of which varies from one grid cell to another (the total depth varies from 0.8 to 3 m); and the SAC-SMA model has five conceptual soil storages with total storage capacity (not depth, which is not specified in the model), which

varies from 20 to 600 mm over the CONUS. For the Catchment model, we took soil depths from the State Soil Geographic Database (STATSGO), and soil texture was adopted from the Food and Agriculture Organization. The soil depth in the Catchment model varies from 1.0 to 1.52 m as in Wang et al. (2009).

Because the soil water holding capacity influences water storage and persistence of SM (Houborg et al. 2012; Xia et al. 2017), and hence arguably drought identification, we evaluated the effect of changes in the soil depths in the Catchment model using an alternate set of soil depths. In particular, we increased the soil depth in the Catchment model to 2 m everywhere and reran the model. We labeled that run as Catm2m as contrasted with the base run, which we labeled Catm. We compared the implications of the differences in soil depth in Catm and Catm2m for drought characteristics over the CONUS below.

Over the northern and western portions of the CONUS, snowmelt is an important water source (Mote et al. 2016). Therefore, we used monthly mean total moisture storage (TMS), which is the sum of SM and SWE instead of SM alone, as in Xiao et al. (2016). We then expressed total moisture storage as percentiles (TMP). In warm regions, soil moisture percentiles (SMP) and TMP are essentially identical. We also used the 3-month standardized runoff index (SRI3) derived from runoff (Shukla and Wood 2008; Mo 2008), which has roughly the same time scale as TMS. We expressed SRI3 in percentiles for consistency with TMP.

How persistent are TMS and SRI3? The persistence of TMS and SRI3 differs from one model to other. Because the persistence is associated primarily with the LSMs' deep soil layers, we compute the characteristic time T_o for TMS anomalies and SRI3 for each model, which we show in Fig. 1. The characteristic time is a measure of persistence defined as

$$T_o = 1 + 2\sum_{t=1}^{N}\left(1 - \frac{t}{N}\right)R(t), \qquad (1)$$

where we took $N = 30$, and $R(t)$ is the autocorrelation at lag t (Trenberth 1984). Parameter T_o provides a better index of moisture storage persistence than does the autocorrelation itself (Trenberth 1984). As shown in Fig. 1, T_o varies considerably among models. In general, T_o for SRI3 is larger than T_o for TMS because SRI3 is computed from 3-month means. The Catchment model–based run (Catm) has smaller T_o, and the pattern is less organized than for the other LSMs. Compared with Catm, Catm2m has larger T_o as expected, although the relatively large T_o over the Northeast is unrealistic.

The other three models (VIC, SAC-SMA, and Noah) have relatively large T_o over the West and the Midwest, where the water storage capacity is large and P has low variability. Parameter T_o is smaller over the East because this region generally is wetter, and hence SM variability is larger. For the mean of SM and SRI3, T_o mostly ranges between 15 and 20 months over the West and 5 and 10 months over the East (Figs. 1i–k).

b. *SSTA indices that influence drought over the United States*

The SST dataset we used is the NOAA Extended Reconstructed Sea Surface Temperature (ERSST) version v3b from 1916 to present (Smith et al. 1996). We computed SSTAs as departures from the monthly mean climatology over the period 1916–2013. There are three SSTA modes that influence P over the United States as established by Schubert et al. (2009). The first SST mode is the trend mode (Fig. 2a). Together with its associated principal component (PC; Fig. 2b), the first SST mode is characterized by a general pattern of warming trends in the southern oceans and the North Pacific and the North Atlantic. In addition to the predominant long-term trends, ENSO has a large influence on P over the CONUS (Ropelewski and Halpert 1986, 1989). ENSO is represented by the Niño-3.4 index (Fig. 2c), which is the mean SSTA over the tropical Pacific (5°S–5°N, 120°–170°W). In addition to ENSO, the AMO can also influence P directly (McCabe et al. 2008; Nigam et al. 2011) and indirectly by modulating the impact of ENSO on P (Schubert et al. 2009; Mo et al. 2009). Figure 2d shows the time series of the 6-month running mean of the AMO.

c. *Integrated drought index as a drought indicator*

We have four time series of TMP and SRI3 from each of the LSMs. To facilitate the mapping of drought conditions objectively with classifications similar to the USDM (Svoboda et al. 2002) and to make use of a single index to represent droughts, Mo and Lettenmaier (2014) introduced an integrated drought index (IDI), which is the grand mean of an equally weighted ensemble mean of multiple drought indices, including SRI3 and total soil moisture percentiles from the four LSMs. We remapped the grand mean index to a uniform probability distribution using the empirical cumulative probability distribution function of the percentile average of the contributing indices. This assures that the remapped IDI has the same probability distribution (ranging from 0 to 1) as each of the individual indices. We used IDI as our indicator of drought, along with a persistence requirement. At each grid point, we required that the IDI be less than 0.3 for at least six consecutive months as a

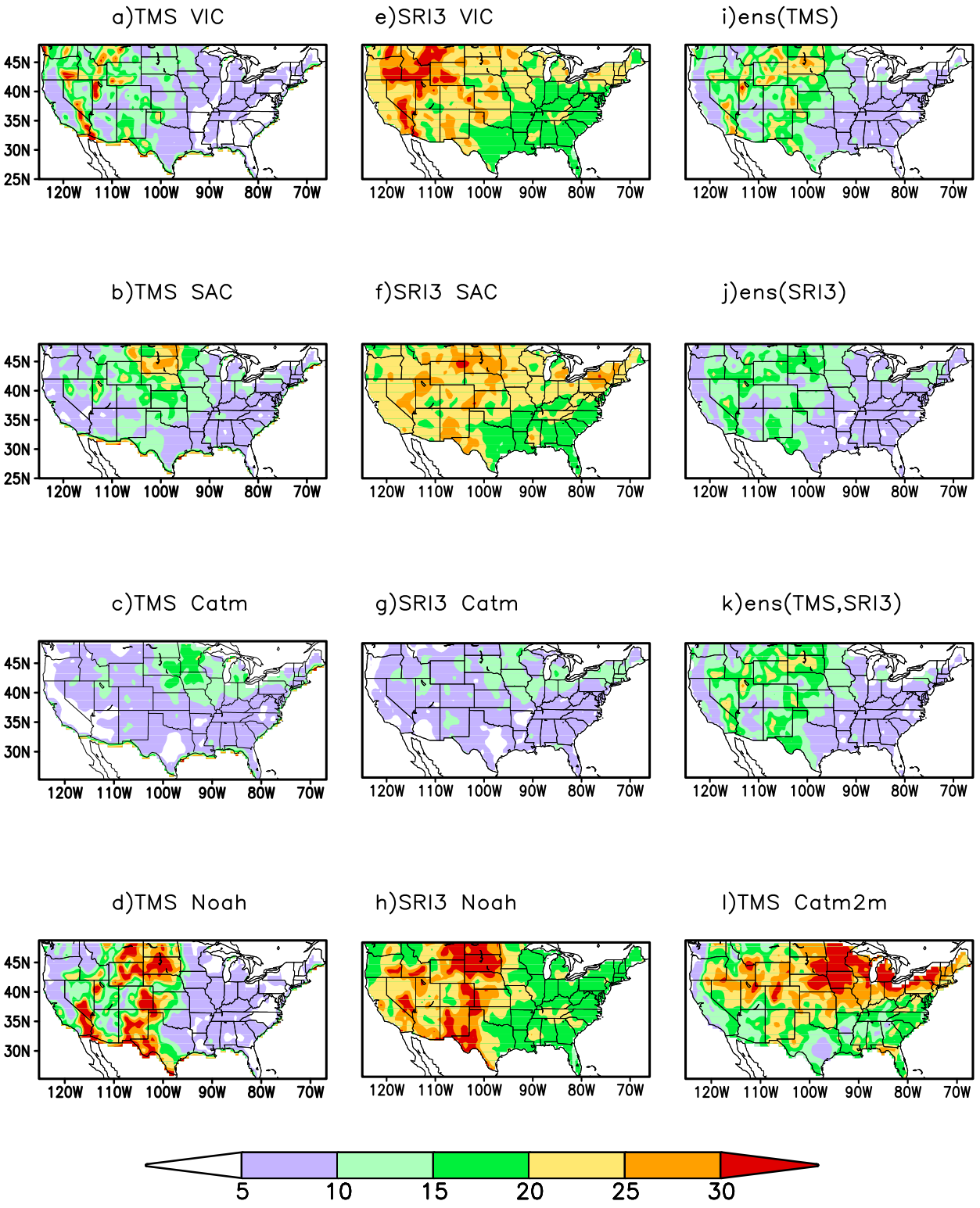

FIG. 1. Parameter T_o for TMS for (a) VIC, (b) SAC-SMA, (c) Catchment, and (d) Noah. (e)–(h) As in (a)–(d), but for SRI3. (i) As in (a), but for the ensemble mean of TMS from four LSMs. (j) As in (i), but for SRI3. (k) As in (i), but for the ensemble mean of TMS and SRI3. (l) As in (a), but for the Catm2m model. Contours are given by the color bar.

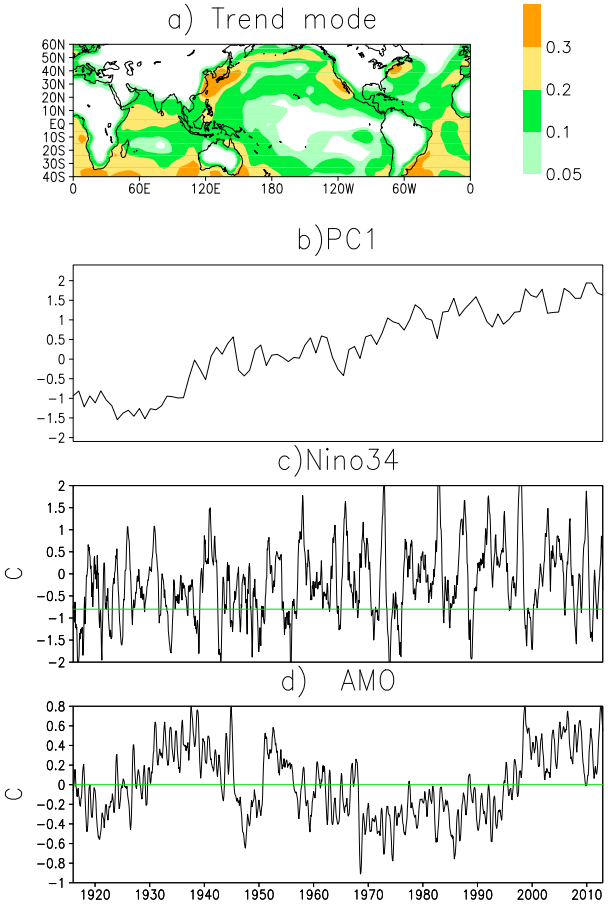

FIG. 2. (a) The first EOF (trend) of the annual mean SSTAs from 1916 to 2013; contours are given by the color bar. (b) PC1 associated with EOF1 and (c) Niño-3.4 index (°C). The green line in (c) denotes that the index value is −0.8. (d) Six-month running mean AMO. The green line in (d) denotes that the index value is zero.

temporal requirement of drought. Using the IDI as our index, we can classify droughts into USDM D0–D4 categories (Svoboda et al. 2002).

For the Catchment models, we computed the time series of the IDIs averaged over the central United States for Catm and Catm2m. Notwithstanding that the T_o values for Catm and Catm2m differ, the time series of mean IDIs averaged over the central United States are quite small (RMSE = 0.025). We decided to use Catm in our subsequent analyses.

To associate circulation anomalies with droughts, we used the monthly mean 500-hPa heights from the Twentieth Century Reanalysis version 2 (Compo et al. 2006, 2011). The dataset has 2° latitude–longitude horizontal resolution. We used the 500-hPa heights for the Northern Hemisphere from 1916 to 2012. Our use of the Twentieth Century Reanalysis was motivated by the fact that it spans the simulation period for the LSMs.

3. Spatial and temporal variations of drought occurrence

a. *Definition of drought*

Many definitions of drought have been suggested. Perhaps the most obvious is a prolonged period of dryness. We define drought events as having the IDI below a threshold (IDI < 0.3) that is equivalent to the USDM D0 threshold and longer than N months ($N = 6$) consecutively, in the interest of focusing on long-term droughts in contrast to flash droughts, which we have addressed previously (Mo and Lettenmaier 2015, 2016).

We define the first time that the IDI falls below the threshold as drought onset X_o, with demise X_d defined as the IDI being above the threshold 2 months consecutively following a drought event (IDI < 0.3 for 6 months or longer). We define a transition period as the month when the P anomaly is negative from prior to drought onset to onset. Our definition is similar to that used by the USDM (Svoboda et al. 2002) but uses the IDI as the indicator.

Figure 3 shows an example for a severe Texas drought in 2010–11. The three-month standardized precipitation index (SPI3), SMP, and SRI3 as well as IDI are averaged over the Texas Gulf region (28°–35°N, 93°–107°W) with SMP and SRI3 derived from VIC model output. Over Texas, SMP and TMP are identical. The negative P anomaly started in September 2010 and ended in November 2011. SMP and SRI3 are shown as an example of drought conditions implied by SM and runoff. Both indices were below 30% for the same period. Although SPI is not a member of the IDI, atmospheric drought sometimes is defined in terms of SPI, so we use it for comparative purposes. SPI was below −0.8 from December 2010 to November 2011. The IDI index agrees with the individual index values and SPI; using the definitions we propose, the drought onset was December 2010 and the demise was November 2011, with transition from September 2010 to December 2010.

b. *Spatial variations of drought occurrence*

Does drought have preferred regions over the CONUS? One of the important features of drought is persistence. By construct, the frequency with which IDI falls below any threshold is identical; what differs spatially is the persistence characteristics of the IDI. For instance, in some cases, the IDI can fall below 30%, but does not persist. If N is the data record length ($N = 98 \times 12 = 1176$ months), then $N_p = N \times 0.3 \sim 352$ months is the number of months that IDI < 0.3. Within the N_p months, there is a subset N_d, which is the number of months under drought (IDI < 0.3 and persists for 6 months or longer). We show in Fig. 4a the percentage of months

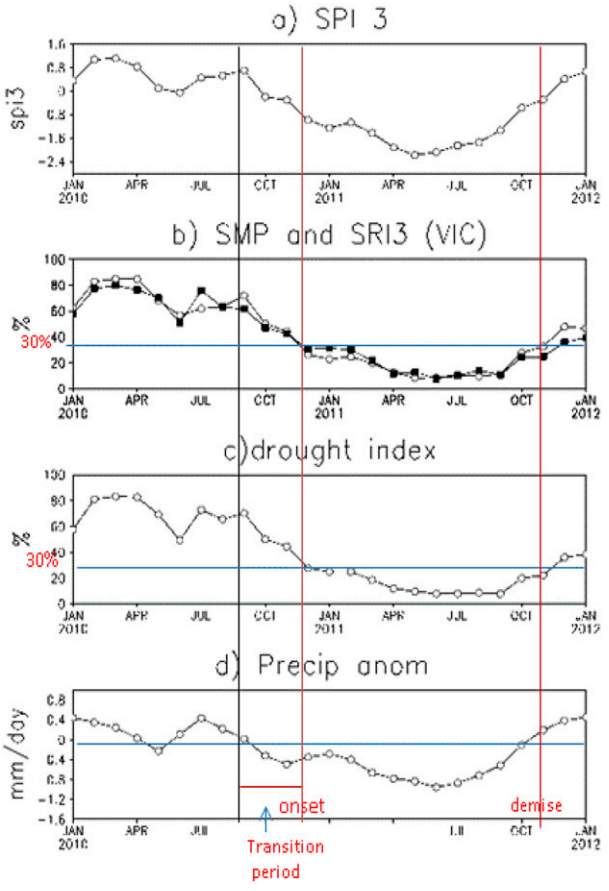

FIG. 3. (a) SPI3 (open circles) averaged over the Texas Gulf region (28°–35°N, 93°–107°W) from January 2010 to January 2012 (dimensionless). (b) As in (a), but for SMP (open circles) and SRI3 (dark circles) from the VIC LSM (dimensionless). (c) As in (a), but for the IDI index (dimensionless). (d) As in (a), but for precipitation anomalies (mm day^{-1}). The red vertical lines denote the onset and demise of the 2010–12 event.

that the IDI persisted for 6 months or longer (N_d/N_p). It shows that low IDI values are more likely to persist over the central United States (30°–42°N, 85°–110°W), with a maximum extending over the Great Plains from Oklahoma and Kansas to South Dakota. Another maximum is located over New Mexico. Drought tends to occur more often and has longer durations in the Great Plains (Fig. 4b). In spring and summer, drought often is accompanied by high temperature. In addition to the decrease of SM due to the lack of P, summer heat adds stress to vegetation growth and leads to further decrease of SM (Koster et al. 2009). Over the relatively dry western interior region, annual precipitation is less than about 1–2 mm day^{-1}, but the West Coast is much wetter, especially from Northern California northward. Over the West Coast, ample (winter) moisture comes from the Pacific via atmospheric river events. For the Pacific Northwest, the percentage of months under drought within N_p months drops to 40% along the coast. The percentage for California is slightly higher, about 50%–60%. For the eastern United States, the percentage of months under drought is less than 60%, with durations on average about 8–10 months. For the areas east of 90°W, moisture comes from the Gulf of Mexico and from the Atlantic. These areas are relatively wet with annual rainfall generally exceeding 3 mm day^{-1}. The percentage of months under drought is lower, and drought once developed is also less persistent.

The CONUS drought record has obvious long-term trends and decadal variability. Drought occurred less often and was less severe later in our study period due to positive trends in P and SM in the twentieth century (Andreadis et al. 2005; Andreadis and Lettenmaier 2006). The IDI shows similar trends. Figure 4c shows the percentage of the areas for which IDI < 0.3 decreases through our period of record (Fig. 4c). As in Andreadis et al. (2005), drought occurrences at the century time scale were dominated by events prior to 1964. The time series of ensemble mean TMS percentiles (TMP) and SRI3 averaged over the central United States shows the percentiles under 30% decrease because both TMP and SRI3 were increasing after 1964. The trends in the IDI are consistent with the trends in TMP and SRI3 percentiles, which are all positive.

In addition to trends, we found that the decadal variability of drought occurrence over the central United States is modulated by the AMO. There is a close association between decadal variations of area covered by drought (Fig. 4c) and the mean SRI3 (Fig. 4d) and TMP (Fig. 4e) over the United States and the AMO (Fig. 2d). There were more areas covered by low IDI and low TMP and SRI3 percentile events when the AMO was positive. For example, the fraction of areas that suffered drought was highest before 1938, in the 1950s, and after 2000. During these periods, the AMO was positive. The percentage of the CONUS covered by drought was less than 30% in the periods 1944–50, 1969–75, 1982–87, and 1990–99, when the AMO was negative.

To assess the statistical significance of trends, we applied the Mann–Kendall test (Hirsch et al. 1982; Hirsch and Slack 1984) to the time series of TMP, SRI3, and the IDI for seasonal means for the period from 1916 to 2013 for each grid point, and results are given in Fig. 5. We colored the increasing trends green and decreasing trends orange. The general patterns shown in Fig. 5 have only modest seasonal variations; the patterns for the different seasons are mostly similar, with increasing trends mostly located over the north-central and Northeast subregions,

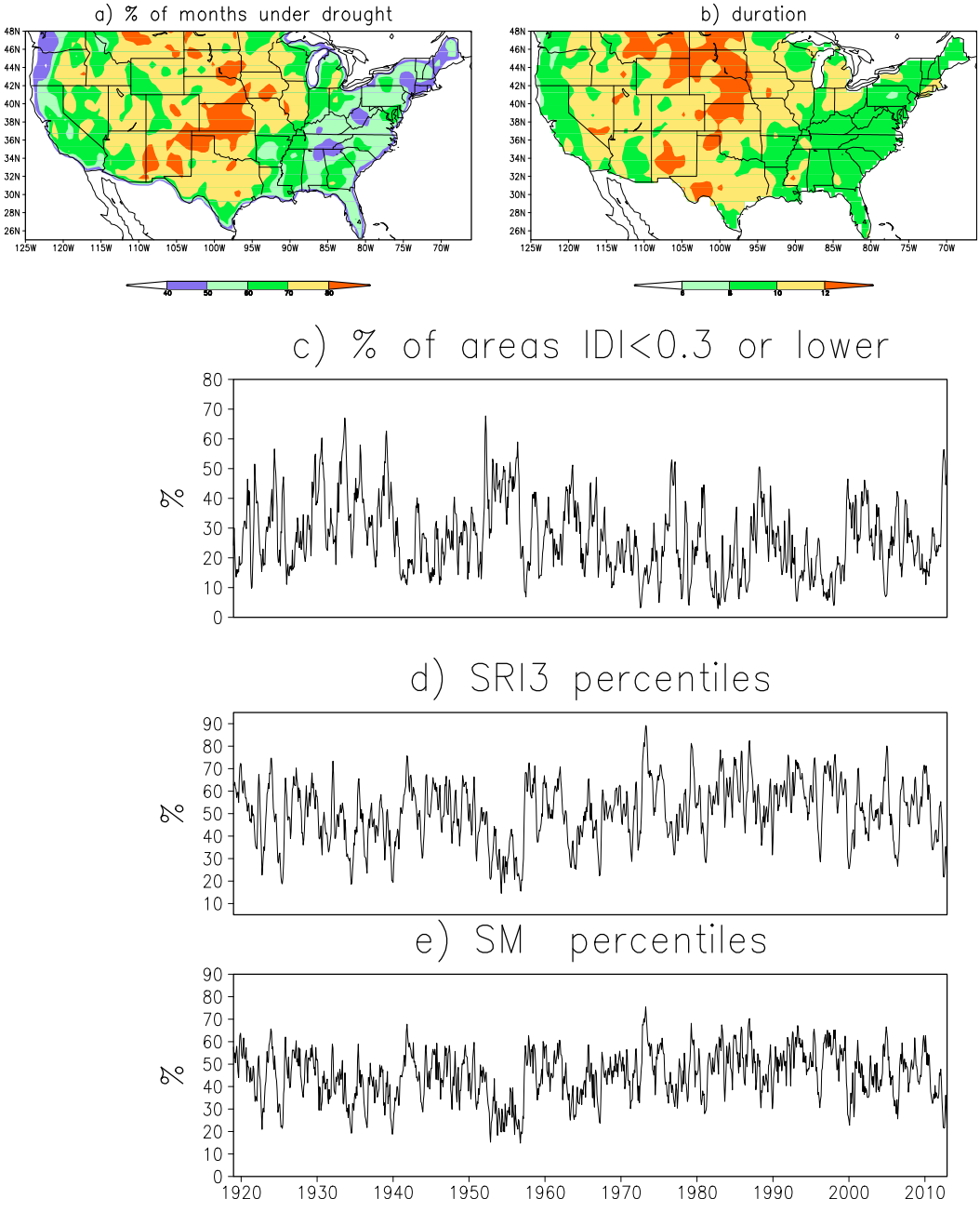

FIG. 4. (a) Percentage of months under drought at each grid point in sequences with IDI < 0.3 persisting for 6 months or longer; contours are given by the color bar. (b) The duration of droughts averaged over drought events in months; contours are given by the color bar. (c) The time series of percentage of areas with IDI < 0.3 over the CONUS, and (d) ensemble mean SRI3 averaged over the Central United States (percentile). (e) As in (d), but for ensemble mean SM percentiles.

where the annual mean precipitation over the same period also had positive trends (Andreadis and Lettenmaier 2006; Lettenmaier et al. 1994). There are negative IDI trends over the Southwest that appear to be mostly attributable to decreasing summer North American monsoon rainfall.

The trends we identified do depend on the analysis period. We performed Mann–Kendall tests on annual mean TMP, SRI3, and IDI for the period 1960–2010, and trends were much weaker, but there are still positive trends over the Northeast and Dakotas and negative trends over part of the Southwest.

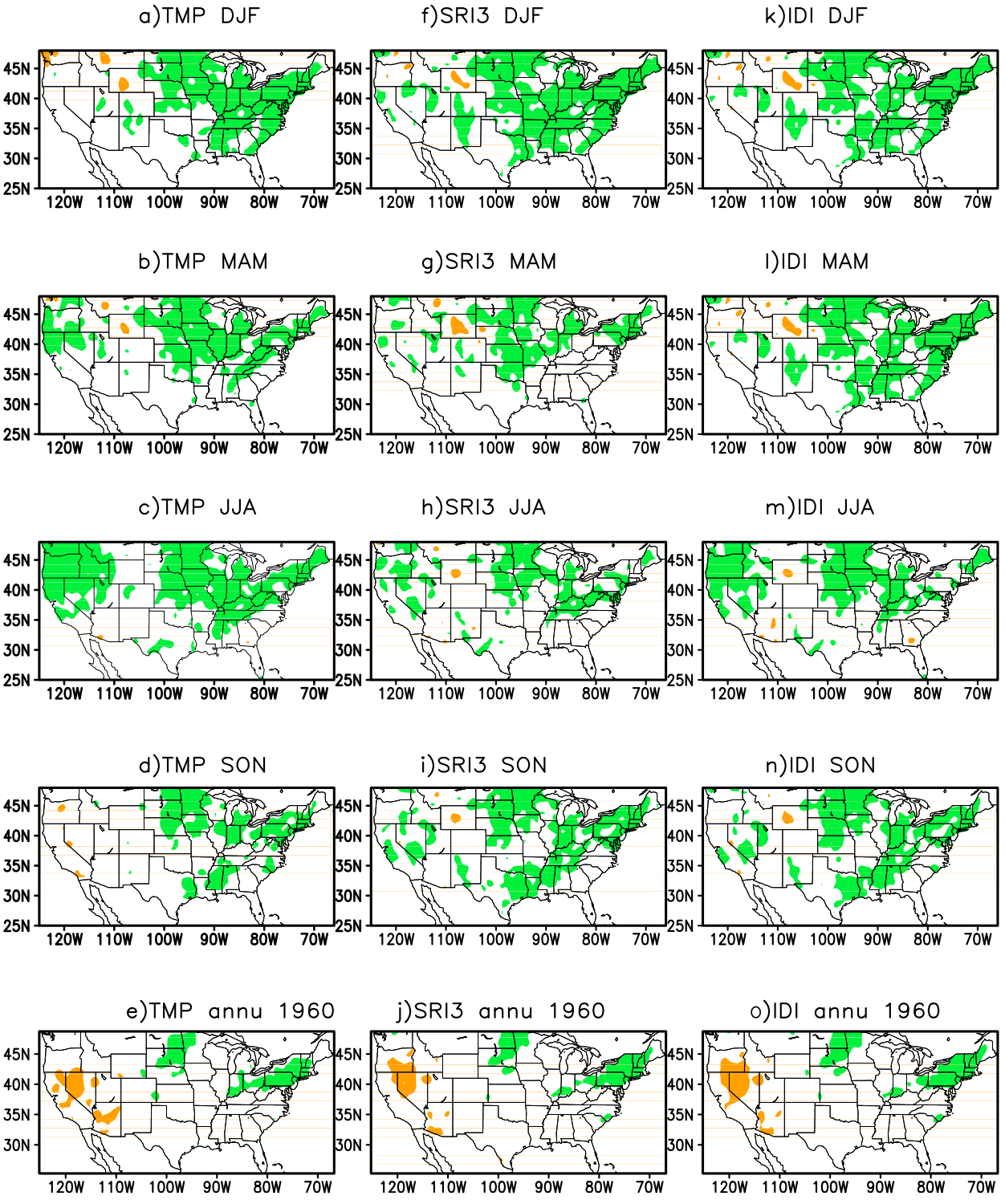

FIG. 5. Mann–Kendall test results for trends in the ensemble mean TMP for (a) December–February, (b) March–May, (c) June–August, (d) September–November, and (e) annual mean from 1960 to 2010. (f)–(j) As in (a)–(e), but for SRI3, and (k)–(o) as in (a)–(e), but for the IDI at each grid point. Areas with statistically significant trends in the variable increasing (decreasing) are colored by green (orange). Mann–Kendall significance level is 0.025 (two-sided test).

TABLE 1. The duration, coverage, and SSTA forcing in the tropical Pacific of the great drought events.

Events	Duration (months)	U.S. under drought mean (%)	Central U.S. under drought (%)			SSTAs in the tropical Pacific
			Mean	Max	Min	
Oct 1917–Aug 1918	11	63	72	89	63	Cold
Sep 1921–Mar 1922	7	49	48	54	35	Cold
Sep 1922–Feb 1923	6	52	70	88	60	Cold
Apr 1925–Sep 1925	6	58	72	84	45	Cold
Jan 1931–Dec 1931	12	60	50	66	21	Cold
Jan 1933–Nov 1934	23	55	56	88	29	Cold
Feb 1936–Dec 1936	11	56	59	80	35	Cold
Sep 1937–Feb 1938	6	49	54	57	36	Cold
May1939–Mar1940	14	62	67	87	42	Warm
Oct 1943–Mar 1944	6	49	54	69	26	Cold
Oct 1952–Mar 1953	6	65	82	96	55	Neutral
Sep 1953–May1955	21	57	74	93	58	Cold
Nov 1955–Mar 1957	17	60	76	93	67	Cold
Apr 1963–Apr 1964	13	52	66	76	45	Warm
May 1988–Oct 1988	6	57	53	56	39	Cold
Apr 2012–Mar 2013	11	62	81	86	48	Neutral

4. Great droughts

a. Identification of great droughts

From Fig. 4c, we selected events for which the area under drought (IDI < 0.3 for 6 months or longer) covered more than 50% of the CONUS, which we define as great droughts. There were a total of 16 events that constituted about 15% of our 98-yr (1916–2013) period of record. The 16 events and their durations are listed in Table 1. After 1964, there were only two great droughts: 1988 and 2012–13.

The IDI averaged over the duration of each of the great drought events except the 2012 event is given in Fig. 6. It should be noted that the mean gives only an approximation of drought location and coverage, because droughts often shift from one location to another, and the area coverage can also change. For each event, we computed the percentages of the entire United States and the central United States that IDI < 0.3 for each month over the duration of drought. We then calculated the mean and maximum and minimum coverages over the duration of that event. Results are given in Table 1. The 2012 event was especially widespread; the mean coverage was about 62% of the CONUS and 81% of the central United States. At its peak, it covered 69% of the CONUS and 86% of the central United States. The minimum coverage over the duration was 48% of the central United States. Its mean areal coverage over the central United States was exceeded only by the 1952–53 event, which was somewhat shorter, and occurred in winter. The mean areal extent over all 16 events was 53% of the CONUS and 64.5% of the central United States.

Since the requirement for great droughts was that 50% of the CONUS be covered, it was expected that many of the droughts would cover some portion of the central United States, because the central United States is at the center of CONUS and about 36% of the CONUS. To test whether the large fraction of great droughts that are at least partly within the central United States essentially was by construct, we performed a Monte Carlo test in which we selected IDI fields from our historical analysis at random times T. We counted the grid points for time T (months) for which IDI < 0.3. If these selected points covered less than 50% of CONUS, then we selected another random time T_1 and counted points for which IDI < 0.3 for the union of the fields for T and T_1. We repeated the process until the total number of grid cells with IDI < 0.3 covered 50% of the CONUS at T_f. We then counted the total number of such grid cells in the central United States for this synthetic "drought" (note that this analysis does not consider duration) at T_f. We repeated this process 100 times, which is roughly the length of the IDI time series. We found that the mean percentage of our simulated points in the central United States was about 52%. In our historic analysis, the fraction was (see Table 1) about 64.5%. Of the 16 great droughts, all except 1921–22 covered more than 50% of the central United States. The 1921–22 event had substantial migration that affected the mean central United States coverage. We conclude, therefore, that the high fraction of central U.S. coverage is not likely to be by construct. We show in Figs. 7a and 7b a composite of the IDI and six-month standardized precipitation index (SPI6) over all of the great drought events, which not surprisingly shows drought centered over the central United States.

From Table 1, the longest of the great droughts occurred in 1933–34 and 1953–55. Both events lasted more than 20 months. While the 2012 event was more widespread, it was much shorter (11 months). Other widespread events over the historical record such as 1931, 1939–40, 1955–57,

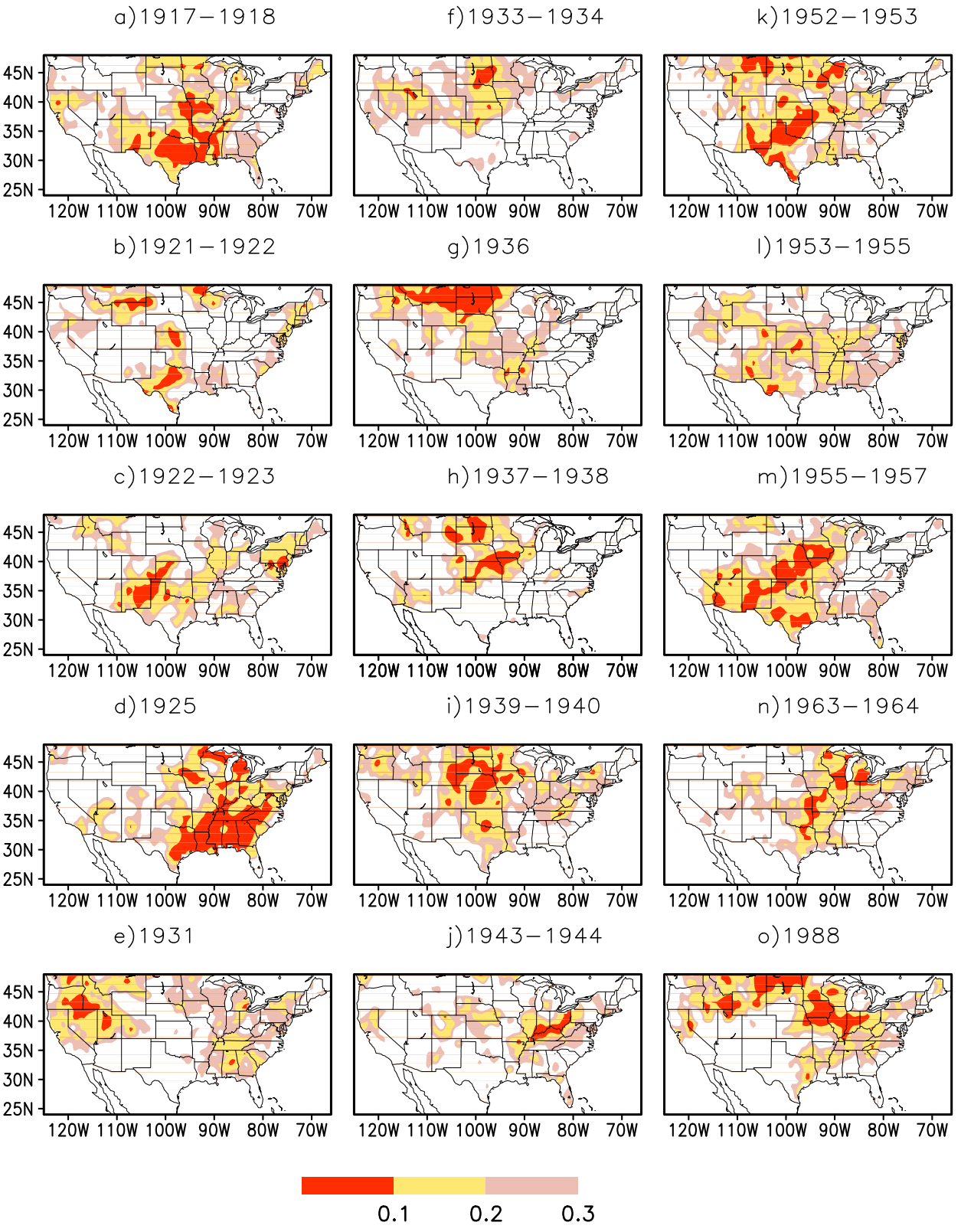

FIG. 6. IDI averaged over the duration of each event listed in Table 1 (except the 2012 event), with areas for which IDI < 0.3 colored.

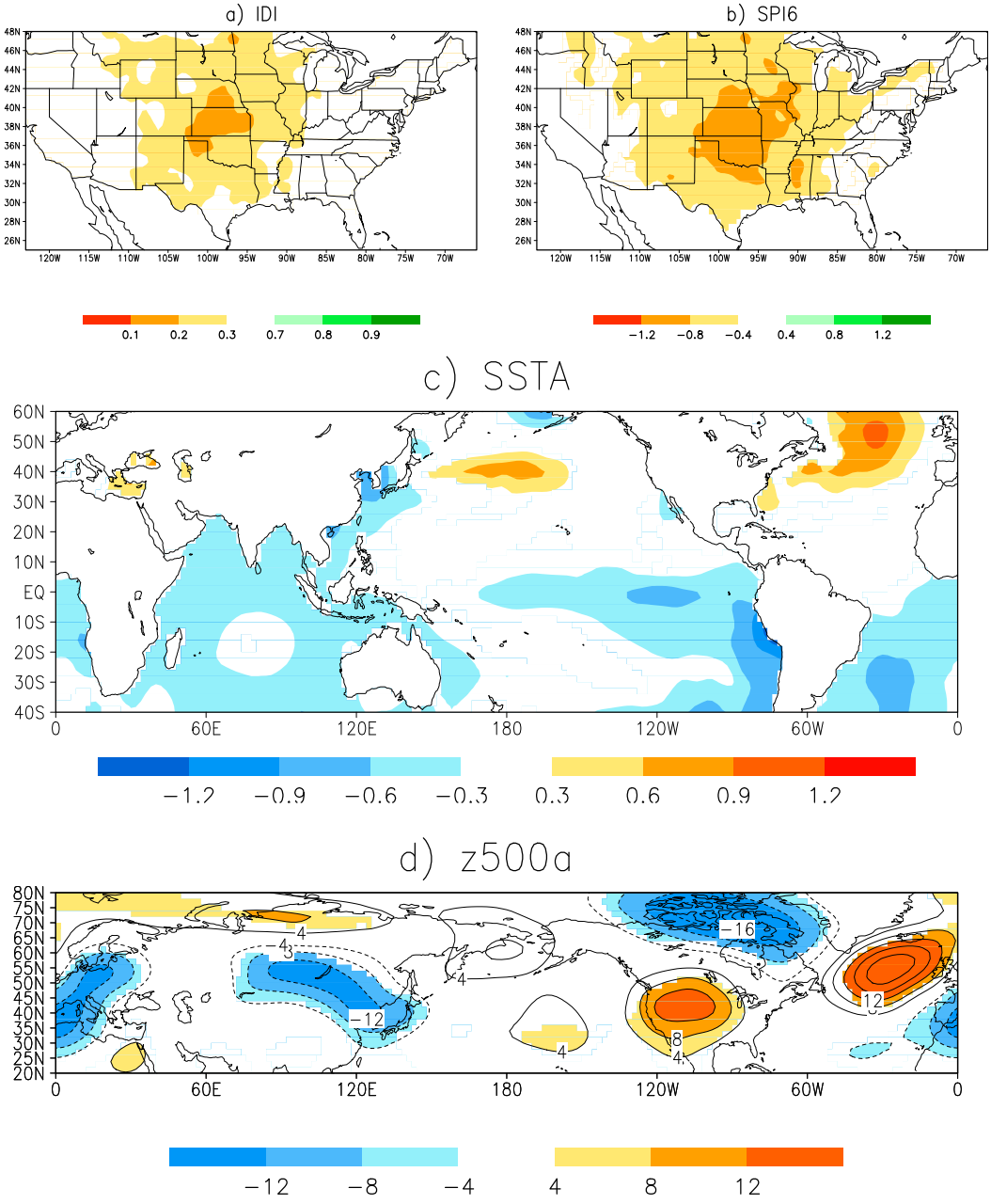

FIG. 7. (a) Composite of IDI for all events listed in Table 1. Contours are given by the color bar. (b) As in (a), but for SPI6. (c) As in (a), but for mean SSTAs for all events associated with cold events listed in Table 1 from season −1 to onset (°C). (d) As in (c), but mean 500-hPa height anomalies (m) with zonal means removed and averaged over the duration of droughts. Areas where the composite is statistically significant at the 5% level are colored. The statistical significance was assessed by the Student's *t* test assuming each event is 1 degree of freedom.

and 1963–64 had longer durations than the 2012 event. As noted above, the 2012 event was the most severe and widespread in the past 50 years.

b. Association with SSTAs

The 2012 event was attributed to internal atmospheric variability by Hoerling et al. (2014). How many of the great droughts shown in Table 1 are attributable to internal atmospheric variability? Schubert et al. (2004) found that droughts over the northern Great Plains were associated with cold ENSO. We examined the SSTAs averaged over the duration of each of the great droughts. To give an indication of tropical conditions during these droughts, we took the average of SSTAs

over the duration of each event over the tropical Pacific part of the Niño-3.4 area (5°N–5°S, 170°–120°W). We classified the 16 events into three categories: warm (positive SSTA anomalies greater than 0.5°C), cold (negative SSTA anomalies less than −0.5°C), or neutral (anomaly magnitudes less than 0.5°C).

Of the 16 events, 12 occurred during cold ENSO years or periods with negative SSTAs covering a portion of the tropical Pacific. Only two events occurred during warm ENSO years: 1939–40 and 1963–64. There were two events in ENSO neutral years: 1952–53 and 2012–13.

To examine the variations of SSTAs among the 12 events that occurred under cold ENSO conditions, we plotted SSTAs averaged over the duration of each event in Fig. 8. They all show cold SSTAs in the southern oceans so they have large projections onto the trend mode (Fig. 2a). All events also show warm SSTAs in the Atlantic, indicating the influence of the AMO on drought. There are weak warm SSTAs in the North Pacific, but the magnitudes of anomalies are weaker, and the patterns effectively are a combination of the PDO and North Pacific EOF mode (Barlow et al. 2001).

There were cold SSTAs in the tropical Pacific averaged over the 12 events as expected, but the locations of SSTAs vary. All events had SSTAs in the tropical Pacific Niño-3.4 region. Some events also had SSTAs in the eastern Pacific. For some events, both locations of drought and SSTAs evolved during drought event. For example, cases such as 1925 and 1931 had cold SSTAs in the tropical Pacific at the beginning of the event. However, when SSTAs diminished, drought persisted. Therefore, the mean over the duration of the event did not show large SSTAs in the tropical Pacific.

The SSTA pattern averaged over the 12 events one season before the occurrence of drought (Fig. 7c) shows the same SSTA pattern as the SSTAs for each event (Fig. 8). This suggests that the SSTA pattern set up one season before drought. The atmospheric responses are related to the mean 500-hPa height anomalies. We computed the mean 500-hPa height anomalies with zonal means removed for the duration of each event and then averaged over the 12 events. The mean height anomaly (Fig. 7d) indicates positive height anomalies were centered over the central United States. This atmospheric pattern tends to block moisture transport by the low-level jet from the Gulf of Mexico to the central United States. Because there is reduced moisture transport, drought events are likely to occur, as indicated by the composites of IDI and SPI6 (Figs. 7a,b). These composites (Figs. 7c,d) suggest that most drought events over the central United States are driven by SSTAs. In that sense, the 2012 event was different from most other central U.S. drought events—it occurred under neutral tropical Pacific SSTAs, in common with only one other event (1952–53) of the 16 events.

Even though the composite of SSTAs indicates that cold ENSO events during the warm phase of the AMO are conducive to the occurrence of drought over the central United States, the SSTAs alone do not lead to the occurrence of drought. We composited the IDI over periods when the Niño-3.4 index was less than −0.8 and the SSTAs in the North Atlantic were positive. The composite does not show drought (IDI < 0.3) over the central United States. In addition to SSTAs, it appears that land surface conditions including P and SM anomalies prior to drought are also important factors for drought to occur.

c. *Transition period*

How long is the transition period? We defined the transition period as beginning when the P anomaly turns negative and ending at the onset of drought. We constructed composites of P and 2-m temperature T_{2m} anomalies from 3 months to drought onset, duration, and demise for events listed in Table 1 (Fig. 9). On average, the P deficit signal starts 2–3 months before drought onset. From month −1 to onset, the composite shows that negative P anomalies extend from the Gulf of Mexico to the Great Plains. The path generally follows the path of the low-level jet. The maximum P deficits occurred from 1 month before onset to onset essentially by construct, because P deficits are needed for drought to occur. Therefore, the transition period typically is 1–2 months. The P deficits averaged over the duration of drought are less than those during onset, because P deficits decrease before the demise phase and P is needed to end drought.

The 2012 drought was accompanied by heat waves. Were such strong droughts always associated with warm temperatures, as suggested by Madden and Williams (1978), Zhao and Khalil (1993), and Trenberth and Shea (2005)? We examined composites of T_{2m} over the duration of drought for events listed in Table 1. For droughts that mostly occurred during winter, there is no significant warming. This could be because both T_{2m} and P are more likely controlled by circulation patterns rather than land surface and atmospheric interactions in winter. For events that occurred mostly from spring to early autumn, we found that warm temperatures occurred over at least a portion of the drought areas over the duration of the events. The physical mechanisms could be similar to those discussed by Koster et al. (2009) and Mo and Lettenmaier (2016). The lack of P decreases SM. Over the central United States, there is a roughly linear relationship between evapotranspiration (ET) and SM. ET decreases lead to sensible heat

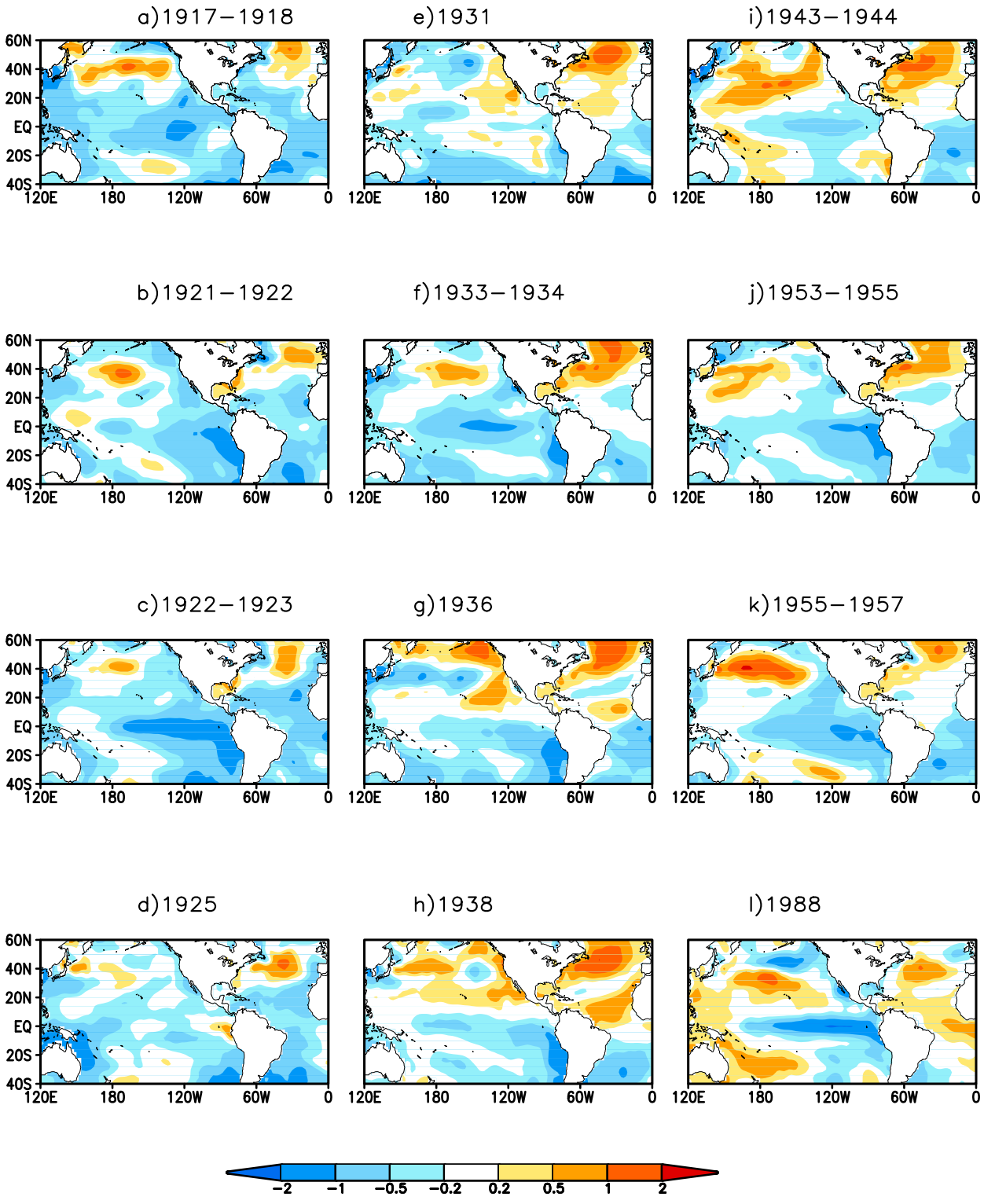

FIG. 8. Mean SSTAs for all cold ENSO events listed in Table 1: (a) 1917–18, (b) 1921–22, (c) 1922–23, (d) 1925, (e) 1931, (f) 1933–34, (g) 1936, (h) 1938, (i) 1943–44, (j) 1953–55, (k) 1955–57, and (l) 1988. Contours are given by the color bar (°C).

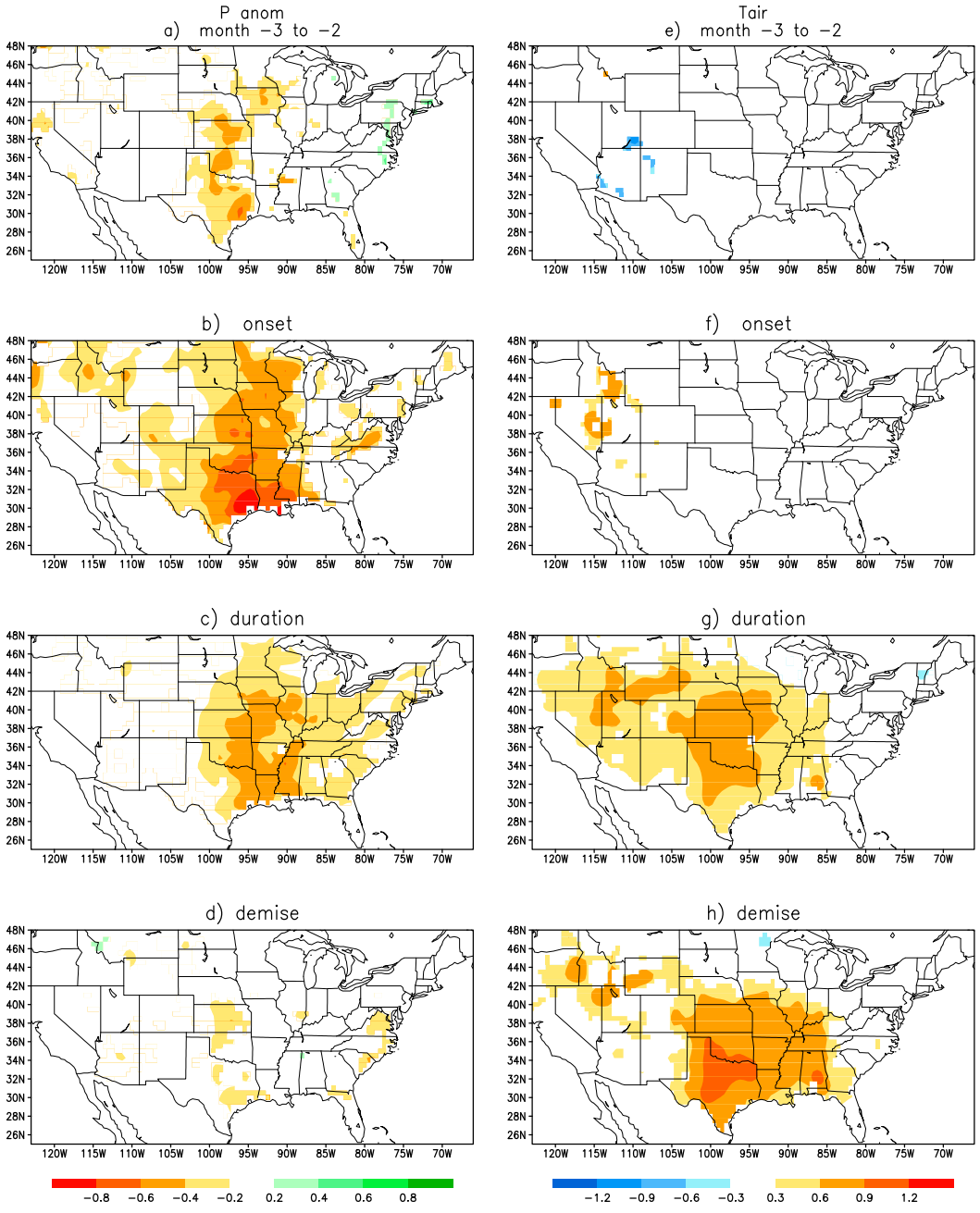

FIG. 9. Composite of P anomalies (mm day^{-1}) from (a) months −3 to −2, (b) month −1 to onset, (c) duration, and (d) demise for all drought events listed in Table 1. The contour interval is given by the color bar. (e)–(h) As in (a)–(d), but for T_{2m} anomalies (°C).

increases that balance the decrease of ET and lead to warmer temperatures. In addition to land–atmosphere interactions, dryness also is usually accompanied by anomalous sunshine hours and less evaporative cooling, as pointed out by Trenberth and Shea (2005). Over the central United States, summer drought is likely to be accompanied by heat waves. In that sense, the 2012 event was similar to other great drought events.

Do the great droughts have a preferred time to occur? That depends on the location of drought and P climatology. For each calendar month, we computed the percentage of all drought events over the central United States that had onset or demise in that month. We averaged over the longitudes (85°–110°W) or latitudes (30°–42°N) over the central United States to examine the seasonal dependence

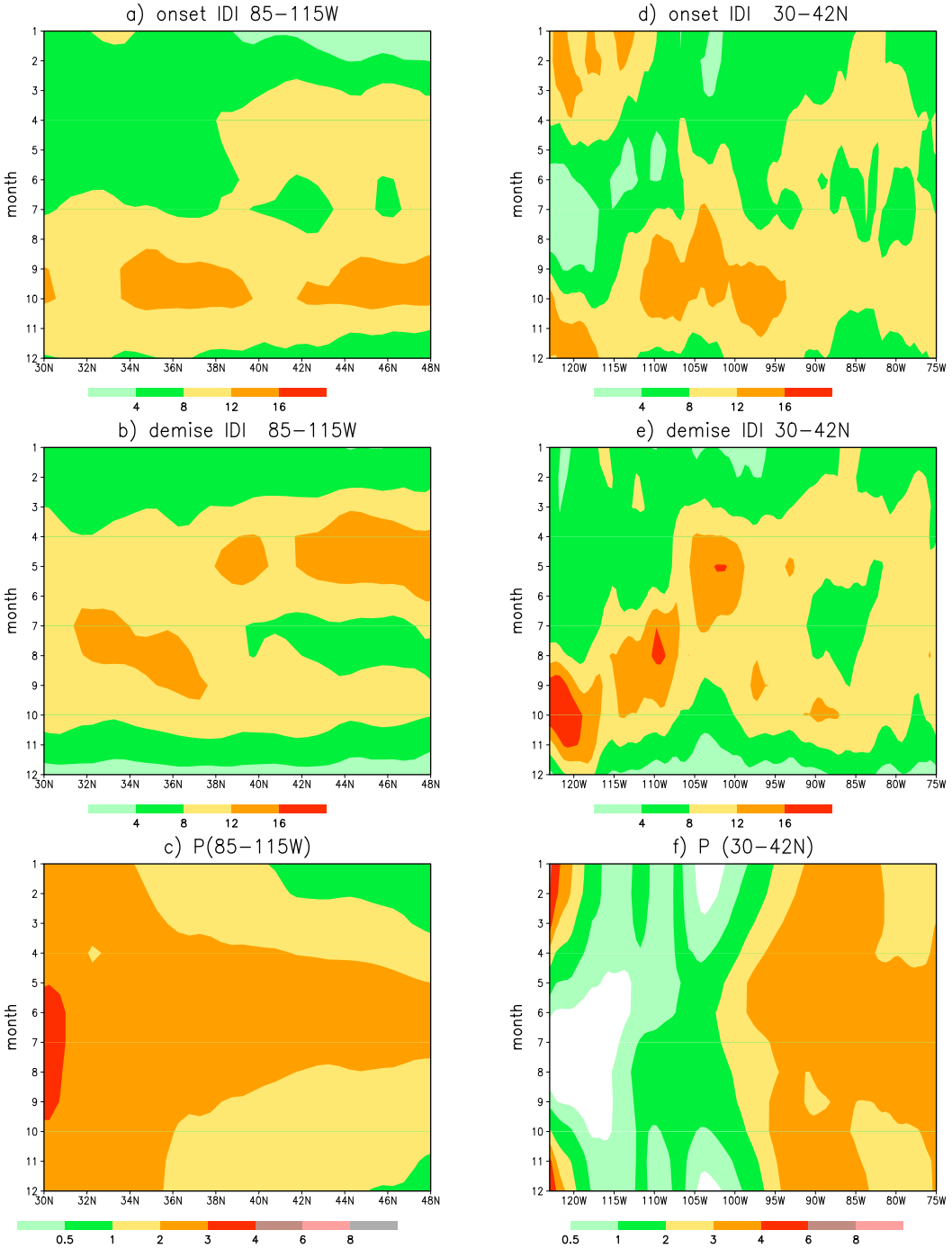

FIG. 10. (a) Time–latitude plot for percentage of drought events over the central United States that had onset at a given month averaged over longitudes (85°–110°W). (b) As in (a), but for drought demise, and (c) as in (a), but for *P* climatology. (d)–(f) As in (a)–(c), but for percentage of drought events that had onset at a given month averaged over latitudes (30°–42°N).

(Fig. 10). The rainy season in the central United States is from April to September. It appears that drought onset is mostly like to occur at the end of rainy season. If drought occurs after a dry rainy season, it tends to persist because rain is unlikely to occur before April. Not surprisingly, the demise of drought is most likely to occur at the beginning of the rainy season.

5. Conclusions

We examined drought variability over the CONUS using gridded observed P and reconstructed TMP and runoff from four land surface models. We used the integrated drought index (IDI) of Mo and Lettenmaier (2014) to define droughts. The IDI is uniformly distributed by construction; hence, the defining characteristics of droughts are associated with temporal and spatial persistence. In particular, we define drought periods as occurring when IDI < 0.3 for 6 months or longer. This requirement shapes the events that we analyzed. We examined great drought events that covered more than 50% of the CONUS and compared them with the 2012 drought. In summary:

- The 2012 drought event was not unique. There were 16 great drought events in the 98 years of record that we analyzed.
- Great droughts occurred less often, and events were less severe as time progressed. Great drought events mostly were located over the central United States, and all but two occurred before 1964.
- All 16 great drought events occurred when the North Atlantic was warm.
- As for the relationships between great droughts and ENSO, two events occurred in a warm ENSO year and two events, including the 2012 one, occurred during a neutral ENSO. The majority of events were associated with cold SSTAs in the Pacific.

All events were associated with warm Atlantic SSTAs. However, droughts did not occur for all periods with warm SSTAs in the Atlantic and cold ENSO in the tropical Pacific. In addition to SSTAs, we found that land surface conditions are important to drought development. In particular, we found that large P deficits tended to occur prior to the onset of drought that was also emphasized by Livneh and Hoerling (2016). These P deficits set up dry surface conditions for droughts to occur.

Acknowledgments. This work was funded by Grant GC-14-189A from NOAA's Modeling, Analysis, and Prediction Program (MAPP) to NOAA's Climate Prediction Center, and by NOAA/MAPP Grant NA16OAR4310139 to the University of California, Los Angeles. The soil moisture and runoff data from the LSMs are available on request to Dr. Lettenmaier at UCLA.

REFERENCES

Andreadis, K. M., and D. P. Lettenmaier, 2006: Trends in 20th century drought over the continental United States. *Geophys. Res. Lett.*, **33**, L10403, https://doi.org/10.1029/2006GL025711.

——, E. A. Clark, A. W. Wood, A. Hamlet, and D. P. Lettenmaier, 2005: Twentieth century drought in the conterminous United States. *J. Hydrometeor.*, **6**, 985–1001, https://doi.org/10.1175/JHM450.1.

Barlow, M., S. Nigam, and E. H. Berbery, 2001: ENSO, Pacific decadal variability, and U.S. summertime precipitation, drought and stream flow. *J. Climate*, **14**, 2105–2128, https://doi.org/10.1175/1520-0442(2001)014<2105:EPDVAU>2.0.CO;2.

Bohn, T. J., B. Livneh, J. W. Oyler, S. W. Running, B. Nijssen, and D. P. Lettenmaier, 2013: Global evaluation of MTCLIM and related algorithms for forcing of ecological and hydrological models. *Agric. Forest Meteor.*, **176**, 38–49, https://doi.org/10.1016/j.agrformet.2013.03.003.

Burnash, R. J. C., R. L. Ferral, and R. A. McGuire, 1973: A generalized streamflow simulation system: Conceptual modeling for digital computers. Joint Federal-State River Forecast Center, NWS, and California Department of Water Resources Tech. Rep., 204 pp.

Cayan, D. R., and K. T. Redmond, 1994: ENSO influences on atmospheric circulation and precipitation in the western United States. *Proc. 10th Annual Pacific Climate (PACLIM) Workshop*, Pacific Grove, CA, California Department of Water Resources, 5–26.

Coats, S., B. I. Cook, J. E. Smerdon, and R. Seager, 2015: North American pancontinental droughts in model simulations of the last millennium. *J. Climate*, **28**, 2025–2043, https://doi.org/10.1175/JCLI-D-14-00634.1.

Compo, G. P., J. S. Whitaker, and P. D. Sardeshmukh, 2006: Feasibility of a 100-year reanalysis using only surface pressure data. *Bull. Amer. Meteor. Soc.*, **87**, 175–190, https://doi.org/10.1175/BAMS-87-2-175.

——, and Coauthors, 2011: The Twentieth Century Reanalysis Project. *Quart. J. Roy. Meteor. Soc.*, **137**, 1–28, https://doi.org/10.1002/qj.776.

Cook, B. I., J. E. Smerdon, R. Seager, and E. R. Cook, 2014a: Pan Continental droughts in North America over the last millennium. *J. Climate*, **27**, 383–397, https://doi.org/10.1175/JCLI-D-13-00100.1.

——, R. Seager, and J. E. Smerdon, 2014b: The worst North American drought year of the last millennium: 1934. *Geophys. Res. Lett.*, **41**, 7298–7305, https://doi.org/10.1002/2014GL061661.

Cook, E. R., D. M. Meko, D. W. Stahle, and M. K. Cleaveland, 1999: Drought reconstructions for the continental United States. *J. Climate*, **12**, 1145–1162, https://doi.org/10.1175/1520-0442(1999)012<1145:DRFTCU>2.0.CO;2.

Ducharne, A., R. D. Koster, M. J. Suarez, M. Stieglitz, and P. Kumar, 2000: A catchment-based approach to modeling land surface processes in a general circulation model. *J. Geophys. Res.*, **105**, 24 823–24 838, https://doi.org/10.1029/2000JD900328.

Ek, M. B., K. E. Mitchell, Y. Lin, E. Rogers, P. Grunmann, V. Koren, G. Gayno, and J. D. Tarpley, 2003: Implementation of Noah land surface model advances in the NCEP operational mesoscale Eta model. *J. Geophys. Res.*, **108**, 8851, https://doi.org/10.1029/2002JD003296.

Fuchs, B. A., D. A. Wood, and D. Ebbeka, 2015: From too much to too little: How the central U.S. drought of 2012 evolving out of one of the most devastating floods on record in 2011. Drought Mitigation Center Faculty Publication 118, 99 pp., https://digitalcommons.unl.edu/droughtfacpub/118/.

Gershunov, A., and T. P. Barnett, 1998: Interdecadal modulation of ENSO teleconnections. *Bull. Amer. Meteor. Soc.*, **79**,

2715–2725, https://doi.org/10.1175/1520-0477(1998)079<2715:IMOET>2.0.CO;2.

Groisman, P. Ya., R. W. Knight, T. R. Karl, D. R. Easterling, B. Sun, and J. H. Lawrimore, 2004: Contemporary changes of the hydrological cycle over the contiguous United States: Trends derived from in situ observations. *J. Hydrometeor.*, **5**, 64–85, https://doi.org/10.1175/1525-7541(2004)005<0064:CCOTHC>2.0.CO;2.

Hirsch, R. M., and J. R. Slack, 1984: A nonparametric trend test for seasonal data with series dependence. *Water Resour. Res.*, **20**, 727–732, https://doi.org/10.1029/WR020i006p00727.

——, ——, and R. A. Smith, 1982: Techniques of trend analysis for monthly water quality data. *Water Resour. Res.*, **18**, 107–121, https://doi.org/10.1029/WR018i001p00107.

Hoerling, M. J., J. Eischeid, A. Kumar, R. Leung, A. Mariotti, K. Mo, S. Schubert, and R. Seager, 2014: Causes and predictability of the 2012 Great Plains drought. *Bull. Amer. Meteor. Soc.*, **95**, 269–282, https://doi.org/10.1175/BAMS-D-13-00055.1.

Houborg, R., M. Rodell, B. Li, R. Reichle, and B. F. Zaitchik, 2012: Drought indicators based on model assimilated gravity recovery and climate experiment terrestrial water storage observations. *Water Resour. Res.*, **48**, W07525, https://doi.org/10.1029/2011WR011291.

Hu, Z. Z., and B. Huang, 2009: Interferential impact of ENSO and PDO on dry and wet conditions in the Great Plains. *J. Climate*, **22**, 6047–6065, https://doi.org/10.1175/2009JCLI2798.1.

Kalnay, E., and Coauthors, 1996: The NCEP/NCAR 40-Year Reanalysis Project. *Bull. Amer. Meteor. Soc.*, **77**, 437–471, https://doi.org/10.1175/1520-0477(1996)077<0437:TNYRP>2.0.CO;2.

Keyantash, J., and J. A. Dracup, 2002: The quantification of drought: An evaluation of drought indices. *Bull. Amer. Meteor. Soc.*, **83**, 1167–1180, https://doi.org/10.1175/1520-0477-83.8.1167.

Koren, V., J. Schaake, K. Mitchell, Q. Duan, F. Chen, and J. Baker, 1999: A parameterization of snowpack and frozen ground intended for NCEP weather and climate models. *J. Geophys. Res.*, **104**, 19 569–19 585, https://doi.org/10.1029/1999JD900232.

Koster, R. D., M. J. Suarez, A. Ducharne, M. Stieglitz, and P. Kumar, 2000: A catchment based approach to modeling land surface processes in a general circulation model: 1. Model structure. *J. Geophys. Res.*, **105**, 24 809–24 822, https://doi.org/10.1029/2000JD900327.

——, S. D. Schubert, and M. J. Suarez, 2009: Analyzing the concurrence of meteorological droughts and warm periods, with implications for the determination of evaporative regime. *J. Climate*, **22**, 3331–3341, https://doi.org/10.1175/2008JCLI2718.1.

Lettenmaier, D. P., E. F. Wood, and J. R. Wallis, 1994: Hydro-climatological trends in the continental United States, 1948–1988. *J. Climate*, **7**, 586–606, https://doi.org/10.1175/1520-0442(1994)007<0586:HCTITC>2.0.CO;2.

Liang, X., D. P. Lettenmaier, E. F. Wood, and S. J. Burges, 1994: A simple hydrologically based model of land surface water and energy fluxes for general circulation models. *J. Geophys. Res.*, **99**, 14 415–14 428, https://doi.org/10.1029/94JD00483.

Livneh, B., and M. Hoerling, 2016: The physics of drought in the U.S. central Great Plains. *J. Climate*, **29**, 6783–6804, https://doi.org/10.1175/JCLI-D-15-0697.1.

——, E. A. Rosenberg, C. Lin, B. Nijssen, V. Mishra, K. M. Andreadis, E. P. Maurer, and D. P. Lettenmaier, 2013: A long-term hydrologically based dataset of land surface fluxes and states for the conterminous United States: Update and extensions. *J. Climate*, **26**, 9384–9392, https://doi.org/10.1175/JCLI-D-12-00508.1.

Madden, R. A., and J. Williams, 1978: The correlation between temperature and precipitation in the United States and Europe. *Mon. Wea. Rev.*, **106**, 142–147, https://doi.org/10.1175/1520-0493(1978)106<0142:TCBTAP>2.0.CO;2.

McCabe, G. J., M. A. Palecki, and J. L. Betancourt, 2004: Pacific and Atlantic Ocean influences on multidecadal drought frequency in the United States. *Proc. Natl. Acad. Sci. USA*, **101**, 4136–4141, https://doi.org/10.1073/pnas.0306738101.

——, J. L. Betancourt, S. T. Gray, M. A. Palecki, and H. G. Hidalgo, 2008: Association of multi-decadal sea-surface temperature variability with US drought. *Quat. Int.*, **188**, 31–40, https://doi.org/10.1016/j.quaint.2007.07.001.

McKee, T. B., N. J. Doesken, and J. Kleist, 1993: The relationship of drought frequency and duration to time scales. Preprints, *Eighth Conf. on Applied Climatology*, Anaheim, CA, Amer. Meteor. Soc., 179–184.

——, ——, and ——, 1995: Drought monitoring with multiple time scales. Preprints, *Ninth Conf. on Applied Climatology*, Dallas, TX, Amer. Meteor. Soc., 233–236.

Mitchell, K. E., and Coauthors, 2004: The multi-institution North American Land Data Assimilation System (NLDAS): Utilizing multiple GCIP products and partners in a continental distributed hydrological modeling system. *J. Geophys. Res.*, **109**, D07S90, https://doi.org/10.1029/2003JD003823.

Mo, K. C., 2008: Model-based drought indices over the United States. *J. Hydrometeor.*, **9**, 1212–1230, https://doi.org/10.1175/2008JHM1002.1.

——, and D. P. Lettenmaier, 2014: Objective drought classification using multiple land surface models. *J. Hydrometeor.*, **15**, 990–1010, https://doi.org/10.1175/JHM-D-13-071.1.

——, and ——, 2015: Heat wave flash droughts in decline. *Geophys. Res. Lett.*, **42**, 2823–2829, https://doi.org/10.1002/2015GL064018.

——, and P. D. Lettenmaier, 2016: Precipitation deficit flash droughts over the United States. *J. Hydrometeor.*, **17**, 1169–1184, https://doi.org/10.1175/JHM-D-15-0158.1.

——, J. N. Paegle, and R. W. Higgins, 1997: Atmospheric processes associated with summer floods and droughts in the central United States. *J. Climate*, **10**, 3028–3046, https://doi.org/10.1175/1520-0442(1997)010<3028:APAWSF>2.0.CO;2.

——, J. E. Schemm, and S. H. Yoo, 2009: ENSO and the Atlantic multidecadal oscillation on drought over the United States. *J. Climate*, **22**, 5962–5982, https://doi.org/10.1175/2009JCLI2966.1.

Mote, P. W., and Coauthors, 2016: Perspectives on the causes of exceptionally low 2015 snowpack in the western United States. *Geophys. Res. Lett.*, **43**, 10 980–10 988, https://doi.org/10.1002/2016GL069965.

Nigam, S., B. Guan, and A. Ruis-Barradas, 2011: Key role of the Atlantic Multidecadal Oscillation in 20th century drought and wet periods over the Great Plains. *Geophys. Res. Lett.*, **38**, L16713, https://doi.org/10.1029/2011GL048650.

Rippey, B. R., 2015: The U.S. drought of 2012. *Wea. Climate Extremes*, **10A**, 57–64, https://doi.org/10.1016/j.wace.2015.10.004.

Ropelewski, C. F., and M. S. Halpert, 1986: North American precipitation and temperature patterns associated with the El Nino/Southern Oscillation (ENSO). *Mon. Wea. Rev.*, **114**, 2352–2362, https://doi.org/10.1175/1520-0493(1986)114<2352:NAPATP>2.0.CO;2.

——, and ——, 1989: Precipitation patterns associated with the high index phase of the Southern Oscillation. *J. Climate*, **2**, 268–284, https://doi.org/10.1175/1520-0442(1989)002<0268:PPAWTH>2.0.CO;2.

Schubert, S., M. J. Suarez, P. J. Pegion, R. D. Koster, and J. T. Bacmeister, 2004: Causes of long-term drought in the U.S. Great Plains. *J. Climate*, **17**, 485–503, https://doi.org/10.1175/1520-0442(2004)017<0485:COLDIT>2.0.CO;2.

——, and Coauthors, 2009: A U.S. CLIVAR project to assess and compare the responses of global climate models to drought related SST forcing patterns: Overview and results. *J. Climate*, **22**, 5251–5272, https://doi.org/10.1175/2009JCLI3060.1.

Shukla, S., and A. W. Wood, 2008: Use of a standardized runoff index for characterizing hydrologic drought. *Geophys. Res. Lett.*, **35**, L02405, https://doi.org/10.1029/2007GL032487.

Smith, A. B., and R. W. Katz, 2013: US billion-dollar weather and climate disasters: Data sources, trends, accuracy and biases. *Nat. Hazards*, **67**, 387–410, https://doi.org/10.1007/s11069-013-0566-5.

Smith, T. M., R. W. Reynolds, R. E. Livezey, and D. C. Stokes, 1996: Reconstruction of historical sea surface temperatures using empirical orthogonal functions. *J. Climate*, **9**, 1403–1420, https://doi.org/10.1175/1520-0442(1996)009<1403:ROHSST>2.0.CO;2.

Svoboda, M., D. LeComte, M. Hayes, R. Heim, and K. Gleason, 2002: The Drought Monitor. *Bull. Amer. Meteor. Soc.*, **83**, 1181–1190, https://doi.org/10.1175/1520-0477-83.8.1181.

Trenberth, K. E., 1984: Some effects of finite sample size and persistence on meteorological statistics. Part I: Autocorrelations. *Mon. Wea. Rev.*, **112**, 2359–2368, https://doi.org/10.1175/1520-0493(1984)112<2359:SEOFSS>2.0.CO;2.

——, and D. J. Shea, 2005: Relationships between precipitation and surface temperature. *Geophys. Res. Lett.*, **32**, L14703, https://doi.org/10.1029/2005GL022760.

Wang, A., T. J. Bohn, S. P. Mahanama, R. D. Koster, and D. P. Lettenmaier, 2009: Multimodel ensemble reconstruction of drought over the continental United States. *J. Climate*, **22**, 2694–2712, https://doi.org/10.1175/2008JCLI2586.1.

Wilhite, D. A., 2006: Drought monitoring, mitigation and preparedness in United States: An end to end approach. *WMO Task Force on Social-Economic Application of Public Weather Services*, Geneva, Switzerland, WMO, 23 pp., https://www.wmo.int/pages/prog/amp/pwsp/documents/Wilhite_WMO_Drought_PWS.pdf.

Xia, Y., D. Mocko, M. Huang, B. Li, M. Rodell, K. E. Mitchell, X. Cai, and M. B. Ek, 2017: Comparison and assessment on three advanced land surface models in simulating terrestrial water storage components over the United States. *J. Hydrometeor.*, **18**, 625–649, https://doi.org/10.1175/JHM-D-16-0112.1.

Xiao, M., B. Nijssen, and D. P. Lettenmaier, 2016: Drought in the Pacific Northwest, 1920–2013. *J. Hydrometeor.*, **17**, 2391–2404, https://doi.org/10.1175/JHM-D-15-0142.1.

Zhao, W., and M. A. K. Khalil, 1993: The relationship between precipitation and temperature over the contiguous United States. *J. Climate*, **6**, 1232–1236, https://doi.org/10.1175/1520-0442(1993)006<1232:TRBPAT>2.0.CO;2.